Free-Form Surface Registration Using Surface Signatures

Sameh M. Yamany and Aly A. Farag
Computer Vision and Image Processing Lab, Electrical Engineering Dept.
University of Louisville, Louisville, KY 40292, USA
email: (yamany,farag)@cvip.uofl.edu

Abstract

This paper introduces a new free-form surface representation scheme for the purpose of fast and accurate registration and matching. Accurate registration of surfaces is a common task in computer vision. The proposed representation scheme captures the surface curvature information, seen from certain points and produces images, called surface signatures, at these points. Matching signatures of different surfaces enables the recovery of the transformation parameters between these surfaces. We propose to use template matching to compare the signature images. To enable partial matching, another criterion, the overlap ratio, is used. This representation scheme can be used as a global representation of the surface as well as a local one and performs near real-time registration. We show that the signature representation can be used to match objects in 3-D scenes in the presence of clutter and occlusion. Applications presented include free-form object matching, multimodal medical volumes registration and dental teeth reconstruction from intra-oral images.

I Introduction

The registration process is an integral part of computer and robot vision systems and still presents a topic of high interest in both fields. The importance of the registration problem in general comes from the fact that it is found in different applications including surface matching[1], 3-D medical imaging[2], [3], pose estimation[4], object recognition[5], [6], [7] and data fusion[8].

In order for any surface registration algorithm to perform accurately and efficiently, appropriate representation scheme for the surface is needed. Most of the surface representation schemes found in literature have adopted some form of shape parameterization especially for the purpose of object recognition. One benefit of the parametric representation is that the shape of the object is defined everywhere which enables high level tasks such as visualization, segmentation and shape analysis to be performed. Moreover, such representation allows stable computation of geometric entities such as curvatures and normal directions. However, parametric representation are not suitable to present general shapes especially if the object is not of planar, cylindrical or toroidal topology. Free-form surfaces, in general, may not have simple volumetric shapes that can be expressed in terms of parametric primitives. Dorai and Jain[5] have defined a free-form surface to be *"a smooth surface, such that the surface normal is well defined and continuous almost everywhere, except at vertices, edges and cusps."* Discontinuities in the surface normal or curvature, and consequently in the surface depth, may be present anywhere in a free-form surface. Some representation schemes for free-form surfaces found in literature include the *splash* representation proposed by Stein and Medioni[9], the *point signature* by Chua and Jarvis[10] and *COSMOS* by Dorai and Jain[5]. Recently Johnson and Hebert[7] introduced the *spin image* representation. Their surface representation, comprises descriptive images associated with oriented points on the surface. Using a single point basis, the positions of the other points on the surface are described by two parameters. These parameters are accumulated for many points on the surface and result in an image at each oriented point which is invariant to rigid transformation.

This paper contributes in the developement of a similar surface representation with the exception of using the curvature information rather than the point density to create the signature image. Furthermore, we apply a selection process to select feature points on the surface to be used in the matching process. This reduction process solves the long registration time reported in the literature, especially for large surfaces. Our technique starts by generating a signature image capturing the surface curvature information seen from each feature point. This image represents a signature of the surface at that point due to the fact that it is almost unique for each point location on the surface. Surface registration is then performed by matching signature images of different surfaces and hence finding corresponding points in each surface. For rigid registration, three point correspondences are enough

This work was supported in part by grants from the NSF (ECS-9505674) and the DoD under contract: USNV N00014-97-11076.

0-7695-0164-8/99 $10.00 (c) 1999 IEEE

to estimate the transformation parameters. This paper is organized as follows. The signature representation is described in section II. The points selection process is introduced in section III and the matching process in section IV. Results and discussions are given in section V and the paper concluded in section VI.

II Surface Signature Generation

Our approach for fast registration is to establish a "surface signature," for selected points on the surface, rather than just depending on the 3-D coordinates of the points. The idea of obtaining a "signature" at each surface point is not new [9], [10], [7]. The signature, computed at each point encodes the surface curvature seen from this point using all other points. This requires an accurate measure of the surface curvature at the point in focus.

For parametric curves or surfaces, curvature measures can be obtained using the *Frenet Frame* values for the case of a curve or the *Weingarten Map* for the case of surfaces[11]. This requires the calculation of curve or surface derivative which is a complex operation and may introduce computational errors to the representation scheme used. Moreover, such measures are hard to obtain for the case of unstructured free-form surfaces. Hebert[12] used a simplex angle to describe changes in a simplex mesh surface. We use the simplex angle to estimate the curvature value at points on a free-form surface.

A free-form surface, in its general form, is composed of unstructured triangular patches. There exists a dual form consisting of unstructured simplex mesh as shown in Fig. 1(a). A topological transformation is used to associate a k-simplex mesh to a k-triangulations or k-manifolds. This transformation works differently for vertices and edges located at the boundary of the triangulation from those located inside. The outcome of this transformation is a (k-p)-cell associated with a p-face of a k-triangulation [13]. In this work, a 2-simplex mesh form is considered in the curvature calculation. Let P be a vertex of a 2-simplex mesh and having three neighbors P_1, P_2, P_3. The three neighboring points define a plane with normal $\vec{U}_P$. They also lie on a circumscribe circle with radius r and the four points are circumscribed by a sphere with center O and radius R as shown in Fig. 1(b). The simplex angle θ shown in Fig. 1(c) is defined as [14]:

$$sin(\theta) = \frac{r}{R} sign(\vec{PP_1} \cdot \vec{U}_P) \qquad (1)$$

This definition is made with the assumption that the three neighbors are linearly independent, thus $r \neq 0$. The simplex angle is related to the mean curvature H

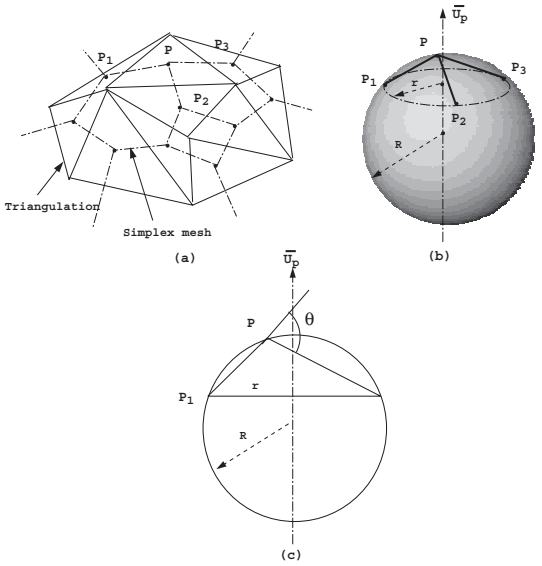

Fig. 1. (a) Duality between triangulation and simplex mesh. (b) The circumsphere of radius R that includes the four points. (c) Cross section of the sphere and the calculation of the simplex angle.

of the surface at the point P as follows:

$$H = \frac{sin(\theta)}{r} \qquad (2)$$

The idea is to use this curvature measure and create a reduced representation of the surface at certain points. This reduced representation encodes the curvature values at all other points and creates an image. This image is called a "signature image" for this point. This is because the change in curvature values with the distribution of all points forming the surface relative to the point in study is unique. This is not true for surfaces of revolution (SOR).

The signature image is generated as follows: As shown in Fig. 2, for each point P, defined by its 3-D coordinates and the normal $\vec{U}_P$, each other point P_i on the surface can be related to P by two parameters: (1) the distance $d_i = ||P - P_i||$ and (2) the angle $\alpha_i = cos^{-1}\left(\frac{\vec{U}_P \cdot (P - P_i)}{||P - P_i||}\right)$. This is a polar implementation of the signature image and it can be easily converted into cartesian form. Also we can notice that there is a missing degree of freedom in this representation which is the cylindrical angular parameter. This parameter depends on the surface orientation which defies the purpose of having an orientation independent representation scheme. The size of the image depends on the object size but for the sake of generalization, each object is normalized to its maximum

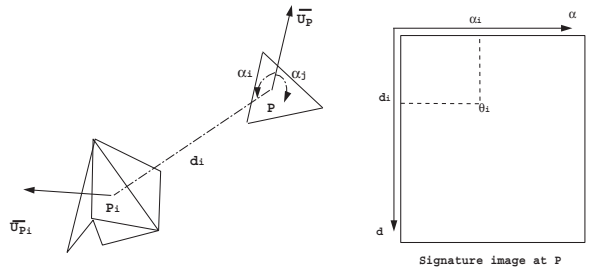

Fig. 2. For each point P we generate a signature image where the image axis are the distance d between P and each other point on the surface and the angle α between the normal at P, $\vec{U}_P$ and the vector from P to each other point. The image encodes the simplex angle θ.

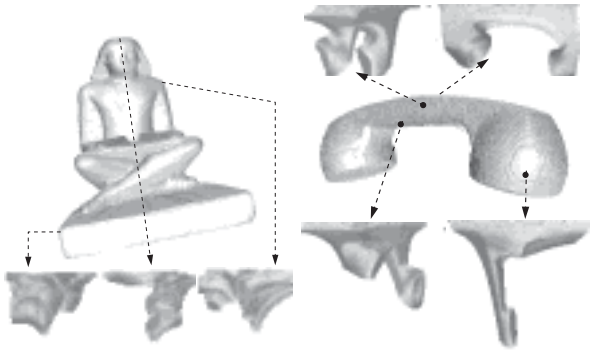

Fig. 3. Examples of signature images taken at different point locations. Notice how the image features the curvature information. The dark intensity in the image represents a high curvature seen from the point while the light intensity represents a low curvature.

length. At run-time matching, the scene-image is normalized to the maximum length of the object in study. At each location in the image the simplex angle θ_i is encoded. Ignoring the cylindrical angular degree results in the case where the same pixel in the image can represent more than one 3-D point on the surface. This usually occurs when the object have surfaces of revolution around the axis represented by the normal at the point P. These points have the same d_i and α_i and lie on the circle that has a radius $d_i cos(\alpha_i)$ and is distant by $d_i sin(\alpha_i)$ from the point P along the axis $\vec{U}_P$. The average of their simplex angles is encoded in the corresponding pixel location.

Figure 3 shows some signature images taken at different points on a statue and a phone handset. Each image uniquely defines the location of the point on the surface due to the encoded curvature information. In SOR, similar images can be obtained for different points. This can be expected as the registration of SOR objects is not unique and has infinite number of solutions.

TABLE I

A AT DIFFERENT λ, THEIR % FROM THE TOTAL M POINTS IN THE MODEL AND THE TIME TAKEN TO OBTAIN THEM ON AN SGI-O2

	statue	statue	speaker	speaker
λ	0.66	0.1	0.3	0.1
$\|A\|$	570	1200	280	1300
M	22541	22541	16150	16150
$\% \frac{\|A\|}{M}$	3%	6%	2%	8%
Time	30sec	30sec	20sec	20sec

III Surface Points Selection

The concept of using special points for registration is not new. Thirion[2] used the same concept to register multimodal medical volumes, and he used "extremal" points on the volume edges (or ridges). Chua and Jarvis[10] used "seeds" points in their matching approach. Stein and Medioni[9] used only highly structured regions in their approach.

In many real life objects, the majority of points forming the surface are of low curvature value. These points are reduntant and do not serve as landmarks of the object. In this work, points of low curvature are eleminated and signature images are only generated for the set of remaing points. A test is also performed to eleminate spike points that have considerable higher curvature than its neighbors. These points are considered as noise.

The simplex angle is used as a criterion to reduce the surface points and use only a subset $A \subset S$ in the registration process, where S is the set of the simplex mesh points.The subset A is defined with respect to a threshold λ such that A contains the landmark regions of the surface.

$$A = \{P_i \in S| \quad |sin(\theta_i)| \geq \lambda, \lambda \geq 0\} \qquad (3)$$

Figure 4 shows two examples of objects and their scanned models. Figure 5 shows the reduced set of points A obtained for each model using different λ and table I summarizes the values obtained. With low threshold values, more details about the object model are considered with considerable reduction in the set cardinality. Even with higher threshold values, most of the landmarks of the object are still present in the set A.

There are two cases, however, where the above analysis will fail. The first is when the surface is a plane or is a piece-wise defined surface (e.g. a cube). In this case for any $\lambda > 0$ the set A will be empty. This can be deduced from Fig. 1(c) when P falls in the plane formed by its neighbors. In this case there exists no

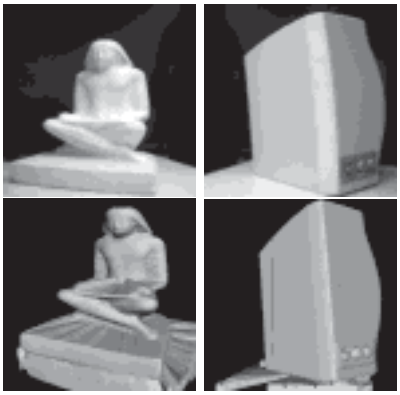

Fig. 4. (Top) Two examples of real objects, a statue and a speaker. (Bottom) Rendered views of the scanned 3-D model of the objects. The statue 3-D model consists of 22541 patches and the speaker 3-D model consists of 16150 patches.

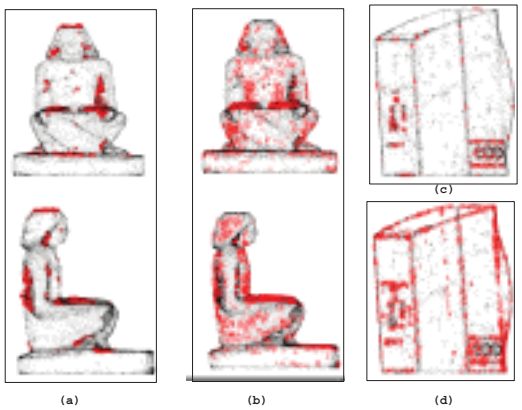

Fig. 5. The reduced set of points obtained for the statue and speaker models using (a) $\lambda = 0.66$, (b) $\lambda = 0.1$, (c) $\lambda = 0.3$ and (d) $\lambda = 0.1$.

sphere circumscribing the four points (i.e. $R = \infty$), thus $H = 0$. The second case is when the surface is part of a spherical, cylindrical or toroidal shape. In this case the curvature measure will be constant over the surface. Fortunalty, in either cases, these surfaces can be easily parameterized and the transformation parameters can be analytically recovered.

IV Signature Matching

The next step in the registration process is to match corresponding signature images of two surfaces/objects or between a 3-D scene and objects in a library. The ultimate goal of the matching process is to find at least three points correspondence to be able to calculate the transformation parameters. The benefit of using the signature images to find the correspondence is the use of image processing tools in the matching, hence reducing the time taken to find accurate transformation. The developed matching engine should be simple based on the fact that the signature images of corresponding points should be identical in their content. Yet, due to the fact that 3-D scanning sensors are noisy in nature and that the 3-D scene may contain clutter or suffer from partial occlusion, a robust matching criteria is needed. One such criteria is *template matching* in which a measure defines how well a portion of an image matched a template. Let $g(i,j)$ be one of our scene signature images and $t(i,j)$ one of the library object (or original surface) signature templates and let D be the domain of definition of the template. Then a measure of how well a portion of the scene image matches the template can be defined as [15]:

$$M(m,n) = \sum_{(j,\ i),(i-m,j-n)\in D} \sum |g(i,j) - t(i-m, j-n)|. \quad (4)$$

For surface signature matching, translation is not needed as the corresponding signature images have the same origin point at (0,0) which means that only $M(0,0)$ is calculated. Another more discriminating measure, based on the standard Euclidean distance, can be:

$$E_n^2 = \frac{1}{N_D^2} \sum_{(j,\ i)\in D} \sum |g(i,j) - t(i,j)|^2. \quad (5)$$

where N_D is the total number of pixels in the domain D. The domain D is defined over the template size. To enable partial matching, the matching measure is augmented by adding the overlap ratio $O = \frac{D_o}{D}$, where D_o is the domain of the overlapping pixels. Figure 6 shows an example of two objects with known transformation parameters and another example where almost half of the object is missing. Table II shows that reducing the size of the signature image leads to a decrease in the number of correct points correspondence which means that more points are needed. Yet, the reduction in time with the smaller size is more suitable for real-time applications. It should be noticed that more reduction in the signature image size may lead to incorrect matching due to the averaging process. The end result of the matching process is a list of groups of likely three point correspondences that satisfy the geometric consistency constraint. The list is sorted such that correspondences that are far apart are at the top of the list. A rigid transformation is calculated for each group of correspondences and the verification is performed using a modified ICP technique[16]. Groups are ranked according to their verification scores, and the best group is refined using the modified ICP technique.

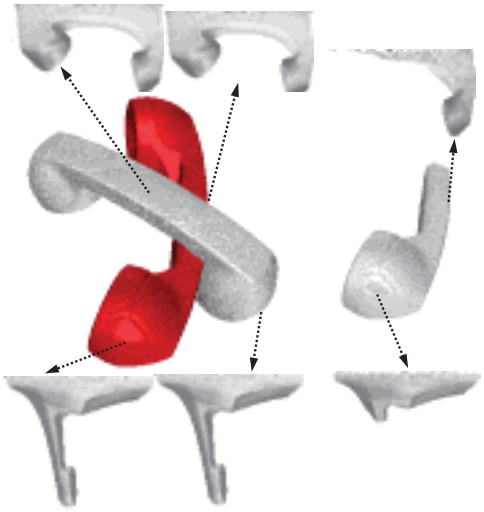

Fig. 6. (a) case 1: Two telephone handsets with known transformation parameters. Notice how similar are the corresponding signature images. (b) case 2: Part of a telephone handset, almost 50% of the original model, and example of the corresponding signature images. Partial matching is needed to establish the correspondence.

TABLE II

COMPARISON IN MATCHING FOR DIFFERENT SIGNATURE IMAGE SIZES

	case 1		case 2	
$A_1 X A_2$	147X147		147X70	
image size	128X128	64X64	128X128	64X64
# of Correct matching	67	40	38	30
Reg. time	54sec	24sec	30sec	10sec

V Results and Discussions

We used the signature implementation in three applications. The first is object registration, an example of which is shown in Fig. 7 where two differently scanned objects are matched together. The signature registration was successful in recovering the transformation parameters. Also the signature representation was used in matching objects in a 3-D scene with their corresponding models in a library. The proximity of the objects in the scene creates large amounts of clutter and occlusion. These contribute to extra and/or missing parts in the signature images. Using the signature polar representation, the effect of clutter, for many points, is only found in the third and/or fourth quadrant of the image as shown in Fig. 8. Examples of such application is shown in Fig. 9. Using the signature matching criterion, all of the models in the scene are simultaneously matched and localized in their correct scene positions. The models in the library and

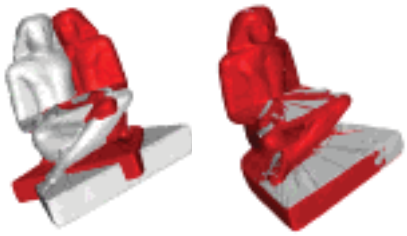

Fig. 7. The signature matching enabled fast recovery of the transformation parameter between these two models.

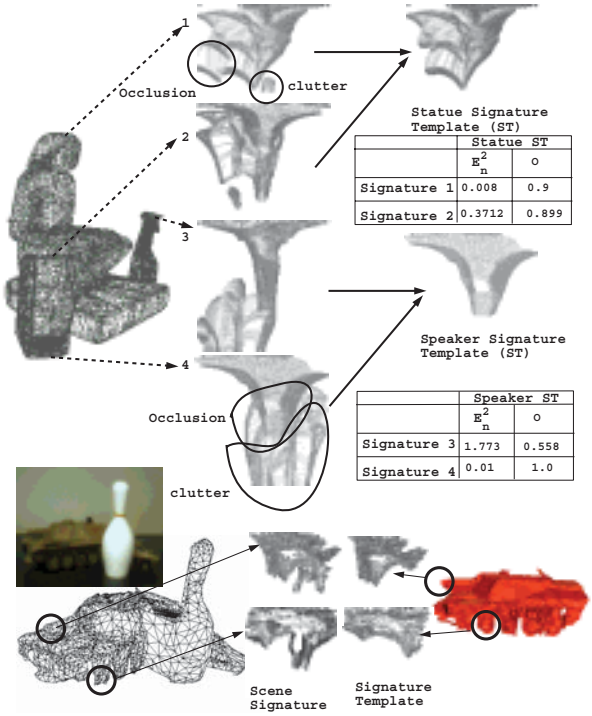

Fig. 8. Illustration of the effect of scene clutter and occlusion on the signature matching.

the 3-D scenes are scanned using a Cyberware 3030 laser scanner with a resolution of 1mm. Some models (e.g. the duck, bell and cup) were obtained from a CAD/CAM library. Table III shows the time needed to match objects in a scene using their signature templates. We compared the performance of our approach with the ICP and the spin image approaches. For the case of matching the statue object, it took 650 seconds using the ICP and 415 seconds using the spin image. Applying the feature points selection process with the spin image, it took 120 seconds to match the object. This is due to the fact that we needed more feature points to match the spin image compared to the points needed to match the signature image. The second application is multimodal medi-

0-7695-0164-8/99 $10.00 (c) 1999 IEEE

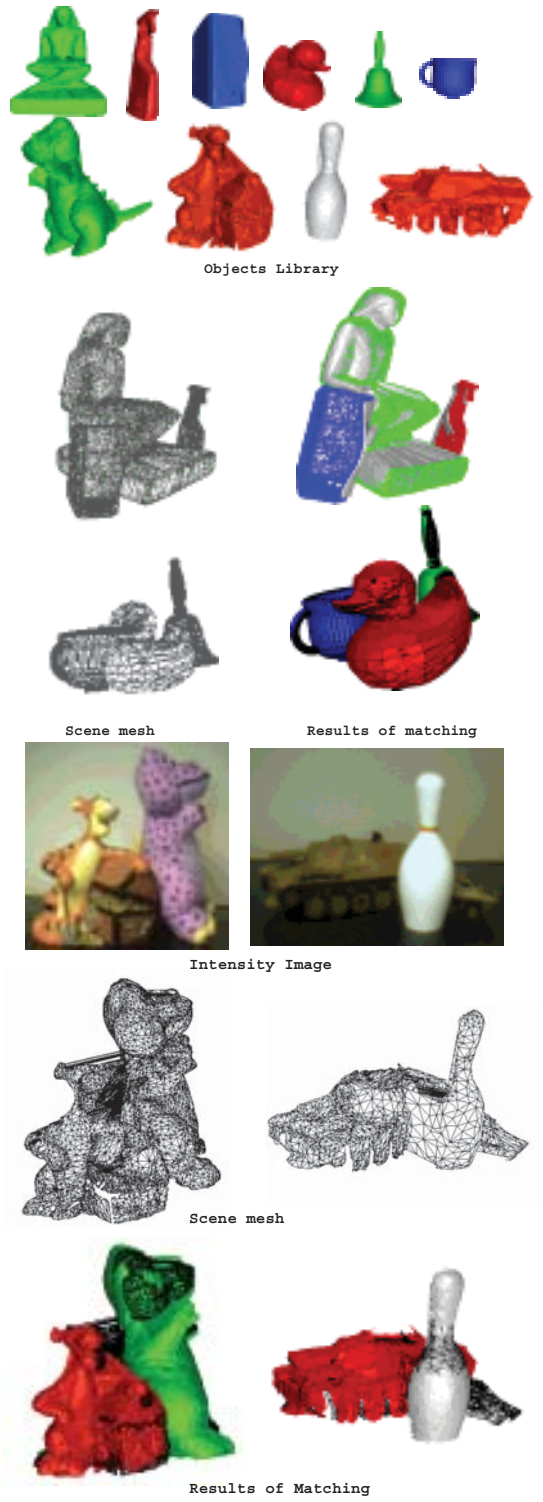

Fig. 9. Examples of using the signature representation in object matching. A library of 10 objects is used. Some of these objects were scanned using a Cyberware 3030 laser scanner with a resolution of 1mm. Others are obtained from CAD libraries.

TABLE III
APPROX. MATCHING TIME IN RECOGNITION ON AN SGI-O2

model	# points	matching time (sec.)
Statue	22541	102
Speaker	16150	87
Bottle	15303	80
Duck	3807	30
Cup	7494	40
Bell	22800	80
Dino	35571	130
Tiger	21606	73
Tank	8619	48
Pin	2110	21

cal image registration as shown in Fig. 10(a). The red surface represents the skin model reconstructed from the MR data and the grey represents the skin model obtained from the CT. These models where obtained using a deformable contour algorithm that finds the outer contour in each slice and reconstructs a 3D mesh by connecting these contours. As the skin is modeled differently in the two image modalities, surface registration will only produce an initial registration. Other techniques like maximizing the mutual information (MI) [17] can be used to enhance the result. The registration using signature and MI was much faster than using MI alone [18]. The third application, shown in Fig. 10(b), is in the dental teeth reconsturction[19], [20]. The overall purpose of this system is to develop a model-based vision system for orthodontics to replace traditional approaches that can be used in diagnosis, treatment planning, surgical simulation and for implant purposes. Image acquisition is obtained using intra-oral video camera and range data are obtained using a 3D digitizer arm. A shape from shading technique is then applied to the intra-oral images. The required accurate orthodontic measurements cannot be deduced from the resulting shape, hence the need of some reference range data to be integrated with the shape from shading results. An neural network fusion algorithm[21] is used to integrate the shape from shading results and the range data. The output of the integration algorithm to each teeth segment image is a description of the teeth surface in this segment. The registration technique is then performed to register the surfaces from different views together.

VI Conclusions

This paper proposed a new surface representation of free-form surfaces and objects. The proposed representation reduces the complexity of the registration and matching problems from the 3-D space into the 2-D image space. This was done by capturing the surface curvature information seen from feature points on the

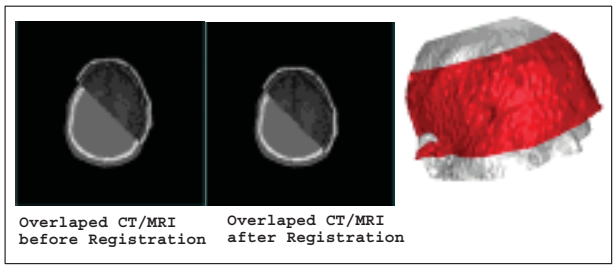

(a) Multimodal Volume Registration

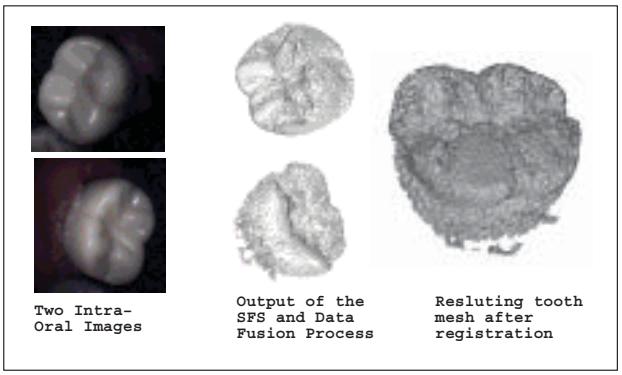

(b) Registration in Dental Application

Fig. 10. Application of the signature representation for (a) Mutlimodal medical volume registration and (b) teeth reconstruction from intra-oral images

surface and encoding it into a signature image. Registration and matching were performed by matching corresponding signature images. The signature images were only generated for selected feature points. The results show a reduction in the registration and matching time compared to other known techniques, a major requirement for real-time applications. Applications included free-form object matching, multimodal medical volumes registration and dental teeth reconstruction from intra-oral images. Currently, we are exploiting the use of the signature representation in scale independent object matching. Regions of same curvature can be detected and segmented in the signature image and scale can be recovered by observing the inter-relationship between segmented curvature regions in different signature images. Future research includes studying the effect of shape deformation on the signature representation and modeling the change in the signature image with a deformation model. This will enable the signature representation to be used in non-rigid registration.

References

[1] Z. Zhang, "Iterative point matching for registration of free-form curves and surfaces," *International Journal of Computer Vision* **13**(2), pp. 119–152, 1994.

[2] J.-P. Thirion, "Extremal points: Definition and application to 3d image registration," *IEEE conf on Computer Vision and Pattern Recognition* , 1994. Seatle.

[3] A. Gueziec and N. Ayache, "Smoothing and matching of 3-d space curves," *International Journal of Computer Vision* **12**(1), pp. 79–104, 1994.

[4] S. Lavallee and R. Szeliski, "Recovering the position and orientation of free-form objects from image contours using 3d distance maps," *IEEE Transactions on Pattern Analysis and Machine Intelligence* **17**, pp. 378–390, April 1995.

[5] C. Dorai and A. K. Jain, "Cosmos-a representation scheme for 3d free-form objects," *IEEE Transactions on Pattern Analysis and Machine Intelligence* **19**, pp. 1115–1130, October 1997.

[6] C. S. Chua and R. Jarvis, "3d free-form surface registration and object recognition," *International Journal of Computer Vision* **17**, pp. 77–99, 1996.

[7] A. Johnson and M. Hebert, "Surface matching for object recognition in complex three-dimensional scenes," *Image and Vision Computing* **16**, pp. 635–651, 1998.

[8] R. Bergevin, D. Laurendeau, and D. Poussart, "Registering range views of multipart objects," *Computer Vision and Image Understanding* **61**, pp. 1–16, January 1995.

[9] F. Stein and G. Medioni, "Structural indexing: Efficient 3-d object recognition," *IEEE Trans. Patt. Anal. Machine Intell.* **14**(2), pp. 125–145, 1992.

[10] C. S. Chua and R. Jarvis, "Point signatures: A new representation for 3d object recognition," *Internation Journal of Computer Vision* **25**(1), pp. 63–85, 1997.

[11] J. Opera, *Differential Geometry and its Applications*, Prentice Hall, 1997.

[12] M. Hebert, K. Ikeuchi, and H. Delingette, "A spherical representation for recognition of free-form surfaces," *IEEE Trans. Patt. Anal. Machine Intell.* **17**(7), p. 681, 1995.

[13] H. Delingette, "Simplex meshes: a general representation for 3d shape reconstruction," Tech. Rep. 2214, Unite de recherche INRIA Sophia-Antipolis, 2004 route des Luciols, BP93,06902 Sophia-Antipolis Cedex (France), Mars 1994.

[14] H. Delingette, M. Hebert, and K. Ikeuchi, "Shape representation and image segmentation using deformable surfaces," *Image and Vision Computing* **10**, pp. 132–144, April 1992.

[15] R. O. Duda and P. E. Hart, *Pattern Classification and Scene Analysis*, John Wiley and Sons, 1973.

[16] S. M. Yamany, M. N. Ahmed, and A. A. Farag, "A new genetic-based technique for matching 3d curves and surfaces," *Pattern Recognition* **32**(10), p. 1817, 1999.

[17] W. M. Wells, P. Viola, H. Atsumi, S. Nakajima, and R. Kikinis, "Multi-modal volume registration by maximization of mutual information," *Medical Image Analysis* **1**, pp. 35–54, March 1996.

[18] A. Eldeib, S. M. Yamany, and A. A. Farag, "Multimodal medical volumes fusion by surface matching," *2nd International Conference on Medical Image Computing and Computer-Assisted Intervention (MICCAI'99), Cambridge, England* , Sept 1999.

[19] M. Ahmed, S. M. Yamany, E. E. Hemayed, S. Roberts, S. Ahmed, and A. A. Farag, "3d reconstruction of the human jaw from a sequence of images," *Proc. IEEE Comp. Vis. and Patt. Recog. (CVPR), Puerto Rico* , pp. 646–653, 1997.

[20] S. M. Yamany, A. A. Farag, D. Tazman, and A. G. Farman, "A robust 3-d reconstruction system for human jaw modeling," *2nd International Conference on Medical Image Computing and Computer-Assisted Intervention (MICCAI'99), Cambridge, England* , Sept 1999.

[21] M. G.-H. Mostafa, S. M. Yamany, and A. A. Farag, "Integrating shape from shading and range data using neural networks," *Proc. IEEE Int. Conf. Comp. Visi. Patt. Recog. (CVPR)* , June 1999. Fort Collins, Colorado.

0-7695-0164-8/99 $10.00 (c) 1999 IEEE